Published in final edited form as:
J Med Primatol. 2014 December ; 43(6): 468–476. doi:10.1111/jmp.12138.

Atypical Nodular Astrocytosis in Simian Immunodeficiency Virus-Infected Rhesus Macaques (*Macaca mulatta*)

Keiko Y. Petrosky[1], **Heather L. Knight**[1], **Susan V. Westmoreland**[1], and **Andrew D. Miller**[2]

[1]Division of Comparative Pathology, New England Primate Research Center, Harvard Medical School, Southborough, MA 01772

[2]Cornell University College of Veterinary Medicine, Department of Biomedical Sciences, Section of Anatomic Pathology, Ithaca, NY 14853

Abstract

Background—Simian immunodeficiency virus (SIV), a model for HIV pathogenesis, is associated with neuropathology.

Methods—Five SIV-infected animals were selected following a database search of 1,206 SIV-infected animals for nodular or astrocytic lesions. 2/5 had neurologic dysfunction and 3/5 were incidental findings.

Results—Histologic examination revealed multifocal nodular foci in the gray and white matter formed by interlacing astrocytes with abundant cytoplasm and large, reactive nuclei. Nodules were often enmeshed with small capillaries. Immunohistochemistry revealed variable immunoreactivity for a panel of markers: GFAP (4/5), vimentin (5/5), Glut-1 (1/5), CNPase (0/5), S100 (5/5), Iba1 (0/5), Ki67 (0/5), and p53 (4/4). *In situ* hybridization failed to detect any SIV RNA (0/5). Immunohistochemistry for simian virus 40, rhesus cytomegalovirus, and rhesus lymphocryptovirus failed to detect any antigen within the lesions.

Conclusion—The immunoreactivity of p53 in the lesions compared to adjacent tissue suggests a local derangement in astrocyte proliferation and function.

Keywords

Histology; immunohistochemistry; GFAP; Vimentin; p53; astrogliosis

Introduction

Human immunodeficiency virus (HIV) mediated immunosuppression may increase the risk for proliferative astrocytic lesions [1-11]. Astrocytic neoplasms including astroblastoma and astrocytoma affect approximately 6% of the HIV patient population [3, 4] compared to <0.005% in the normal population[12]. Moderate to severe perivascular astrocytosis has been reported in simian immunodeficiency virus (SIV) positive individuals [13]. To our knowledge, nodular astroglial proliferative lesions have been rarely reported in SIV-infected nonhuman primates, including a solitary malignant astrocytoma [14] and a proliferative and

Corresponding author keiko_petrosky@hms.harvard.edu.

dysplastic astrocytosis [15], both conditions associated with SV40 CNS infection in the context of SIV-immunosuppression. SIV does manifest multiple other pathologies in the central nervous system, including SIV encephalitis and a variety of neurodegenerative changes [16].

The World Health Organization classifies astrocytic tumors into grades I-IV, with the highest grade (Grade IV) given to glioblastoma multiforme (GBM) [17]. Tumor suppressor p53 is a transcription factor mutated in 50% of tumors and is commonly constitutively expressed in tumors [18]. Alterations of the p53 pathway in GBM include mutations to both upstream and downstream regulators and effectors, as well as mutations in p53 itself; the most common mutations alter expression of genes controlling senescence and apoptosis [19]. The overall result of these mutations includes constitutive expression of mutant p53 [20]. Approximately 33% of low grade infiltrating astrocytoma (Grade I-II) have mutations detected in the p53 gene [17]. Alteration of p53 expression is seen in 60% of diffuse astrocytoma [21], 25-30% of primary GBM, and 60-70% of secondary GBM [22]. Astrocytic neoplasia reported in the rhesus macaque includes radiation-induced GBM [23] and a spontaneously occurring neurohypophyseal astrocytoma [24]. In SIV-infected rhesus macaques, simian virus 40 (SV40) has been directly isolated from malignant astrocytoma [14]; however the role this virus plays in oncogenesis is incompletely understood.

Herein we describe five cases of atypical nodular perivascular lesions in SIV-infected rhesus macaque and detail the histopathologic features, including increased p53 immunoreactivity within the lesions.

Materials and Methods

Retrospective analysis of the New England Primate Research Center (NEPRC)'s database of archived necropsy reports identified 1,206 cases of SIV-infected rhesus macaques from 1997-2012. We identified five cases with nodular lesions in the brain and brainstem following a search for the following key words in the microscopic findings in the central nervous system (CNS): nodule, spindloid, spindle, whorls, astrocytosis, and aggregates of astrocytes. A comparable search of non-SIV-infected rhesus macaques failed to reveal any lesions similar to those presented in this case report. Four out of five cases demonstrated AIDS-defining lesions indicating SIV-immunosuppression. Signalment, SIV variant, inoculation route, days post inoculation, location and size of nodular lesions are indicated in Table 1. All of the animals in this study were housed at the NEPRC in a biosafety level 3 facility and cared for in accordance with the National Research Council's Guide for the Care and Use of Laboratory Animals (8^{th} edition, 2011), the standards of the Harvard Medical School Standing Committee on Animals, and The Association for the Assessment and Accreditation of Laboratory Animal Care.

Representative sections of all major organs were collected, fixed in 10% neutral buffered formalin, and embedded in paraffin. Five μm sections of representative samples were routinely prepared and stained with hematoxylin and eosin (H&E).

To identify cell types, to characterize cellular proliferative processes, and to test for the presence of viral antigens for possible viral etiology, brain tissues were subjected to extensive immunohistochemical analysis. Astrocytes were distinguished through the expression of glial fibrillary acidic protein (GFAP), a class-III intermediate filament highly expressed in mature astrocytes, and the mesenchymal cell marker vimentin, a class-III intermediate filament found in non-epithelial cells [25]. The enzyme 2′, 3′-cyclic nucleotide 3′-phosphodiesterase (CNPase), expressed at high levels by oligodendrocytes in the central nervous system and Schwann cells in the peripheral nervous system, is used as a marker to identify these cell types [26]. S100, a low-molecular weight protein found in cells derived from the neural crest, is expressed in glial cells and is up regulated in reactive astrocytes [27] and expressed in a variety of different cancers [28-30]. Ionized calcium binding adaptor molecule 1 (Iba1) is a marker of microglia/macrophage-lineage cells [31]. Glut-1 is a major glucose transporter in the mammalian blood-brain barrier and is expressed in erythrocytes [32] and endothelial cells in the brain [33]. Aberrant Glut-1 has been shown to correlate with poor survival in a variety of human and canine cancers [34-36]. Antibodies were also used to test for the presence of viral antigens for simian virus 40 (SV40), cytomegalovirus (CMV), and EBV-homologue lymphocryptovirus (LCV).

Formalin-fixed, paraffin-embedded sections were deparaffinized, rehydrated, and blocked with 3% hydrogen peroxide. See Table 2 for detailed immunohistochemistry protocols. Briefly, all steps were followed by washing with Tris-buffered saline. All antibodies except for p53 required blocking with avidin-biotin (Invitrogen Corporation, Frederick, Maryland) prior to blocking with Dako protein block (DakoCyomation, Carpinteria, California) for ten minutes. Following washing with Tris-buffered saline, antigen-antibody complex formation was detected using diaminobenzadine (DAB; DakoCytomation) and counterstained with Mayer's hematoxylin. In all cases, control sections were incubated with isotype-specific irrelevant antibody controls. Positive controls consisted of tissue from brain (GFAP, Glut-1, Iba1, and CNPase), intestine (vimentin, Ki67), pancreas (S100), SIV and SV40 encephalitis, cytomegalovirus (CMV) orchitis, and colon cancer (p53) samples. To prevent irregularities between runs, each immunohistochemical staining was performed in a single batch. Detection of virion-associated RNA by *in situ* hybridization (ISH) for SIV RNA was performed as previously described [37].

Results

Histology

Histologic examination revealed multifocal perivascular nodular foci of variable size (Table 1) in the gray and white matter of various structures of the brain, including the cerebral cortex, globus pallidus, thalamus, and cerebellum, and brain stem (Fig. 1A). The nodules were composed of densely cellular, interlacing plump to elongate spindle cells with abundant eosinophilic cytoplasm and large, reactive nuclei (Fig. 1B). Nodules were often interlaced around small capillaries. In Case 3, effacing the hypothalamus, there was a large focus three mm in diameter (Fig. 1C) composed of multiple coalescing nodules 100-200 μm in diameter (Fig. 1D) with smaller nodules 20-50 μm in diameter surrounding adjacent small capillaries.

Immunohistochemistry

Characterization and phenotype of cells in lesions—To determine the cellular phenotype of the cells within the lesions, brain sections were analyzed using immunohistochemistry using several CNS cell-type specific markers: GFAP and vimentin for astrocytes, CNPase for oligodendrocytes, S100 for histiocytic / dendritic cells and other cells of neural crest origin, IBA-1 for microglia/macrophages, and Glut-1 for endothelial cells. Spindle cells composing the nodular lesions exhibited robust immunoreactivity with a homogenous distribution of cytoplasmic vimentin in all cases (5/5, Figs. 2B, 3B) and cytoplasmic GFAP in four cases (4/5, Figs. 2A, 3A). Additionally, prominent GFAP+ activated astrocytes (gemistocytes) with strong immunoreactivity were present surrounding nodules in all cases. Spindle cells composing the nodular lesions lacked immunoreactivity for CNPase (0/5, data not shown), although occasional CNPase+ oligodendrocyte processes were evident trapped or traversing the lesions. CNPase immunoreactivity was restricted to the white matter in the sections around the lesions. Robust cytoplasmic S100 immunoreactivity was seen in both spindle cells composing the nodular lesions and in S100 immunoreactive microglia (5/5, data not shown). In addition, IBA-1 immunoreactive microglia were present in the nodules; however the proliferative cells had no immunoreactivity (0/5, Fig. 2C, Fig 3C). Most vessels, including capillaries not associated with the nodular lesions, displayed Glut-1 immunoreactivity. Glut-1 immunoreactive endothelial cells were present as numerous small, proliferative capillaries within the nodular lesions (4/5, Fig 2D) and there were profoundly hypertrophic vessels in Case 3 (1/5, Fig. 3D). Results are summarized in Table 3.

Indices of cellular proliferation and cell cycle control—To assess the proliferative nature of the lesions, Ki-67 was used as a marker of mitosis and cellular proliferation. Unexpectedly, the cells in the nodular lesions demonstrated limited Ki-67 immunoreactivity (0/5) (Fig. 4A, C). Since alterations in p53 expression have been associated with astrocytic masses, sections were analyzed for p53. Spindle cells composing the nodular lesions exhibited immunoreactivity with coarsely stippled nuclear localization of p53 in four of four cases available (Fig. 4B, D). 40% of the spindle cells composing the lesions exhibited strong immunoreactivity, while the remaining 60% showed lesser immunoreactivity. Rare cells scattered throughout the white and gray matter exhibited p53 immunoreactivity. Case 1 had insufficient tissue remaining for p53 immunohistochemistry. Percentage of immunoreactive nuclei found within the proliferative lesions, determined by averaging results from five lesions, are shown in Table 4.

Viral detection—SIV viral RNA as well as viral antigens of possible opportunistic CNS viruses (SV40, CMV, and LCV) were examined within the nodular lesions. In situ hybridization for SIV RNA was negative in all sections (0/5, data not shown). SV40 and LCV immunoreactivity were negative in all sections (0/5, data not shown). Immunoreactivity for CMV antigen was negative in the astrocytic foci for all cases, (0/5, data not shown), but Case 3 had occasional isolated meningeal nuclear CMV immunoreactivity distant to the nodular lesions. Results are summarized in Table 3.

Discussion

The cases shown herein demonstrate unique perivascular nodular lesions in the brain of SIV-infected rhesus macaques. The positive immunoreactivity for GFAP and vimentin in the perivascular nodular lesions are consistent with astrocytic origin. The nodular lesions in the outlier, case 3, displays immunoreactivity to vimentin but not GFAP. Given that in vitro cultures of astrocytes typically express only low levels of GFAP, the spindle cells in case 3 may also be astrocytes [38]. Astrocyte activation in response to aberrant endothelial cells is unlikely given the normal appearance of the endothelial cells composing the proliferative capillaries within the nodular lesions in the other four cases.

SIV encephalitis is commonly associated with multinucleated giant cells and occurs in almost a quarter of all SIV-infected macaques [39, 40] . Following SIV infection of macrophage and microglia, the sustained inflammation and release of inflammatory cytokines may lead to astrocytosis [41]; however these nodular lesions have not been previously described as part of the late stage neuroprotective response.

Numerous viruses are known to cause infection and pathology within the central nervous system of SIV-immunosuppressed rhesus macaques. Primary SV40 infection of oligodendrocytes and astrocytes is associated with meningoencephalitis in SIV-infected rhesus macaques [15, 42], while progressive multifocal leukoencephalopathy (PML) has been reported in cases of SV40 recrudescence in oligodendrocytes following SIV infection [15, 43-45]. Rhesus CMV infection of ependymal cells, pia mater, and neurons is associated with meningitis and myelitis in SIV-infected rhesus macaques with AIDS [46]. Of interest, is the recent association of CMV with astrocytic tumors in humans [47, 48]. Primary central nervous system lymphoma, an AIDS-related non-Hodgkin’s lymphoma [49], in SIV-immunosuppressed macaques contain rhesus LCV [50], a virus with 64% homology to human Epstein Barr Virus [51]. Encephalitis has been induced in rhesus macaques with rhesus LCV infected B-cells [52]. None of these viruses were detected within the proliferative astrocytic nodules.

The perivascular nodular astrocytic lesions shown here resemble some features of astrocytic neoplasms seen in HIV-infected patients. The histologic characteristic of a perivascular distribution of the nodular lesions suggests a hematogenous or blood-brain barrier association and it is possible that these lesions are an aberrant response to SIV viremia. The strong immunoreactivity of p53 in the lesions compared to adjacent tissue suggests the local derangement in astrocyte proliferation and function of a pre-neoplastic or neoplastic process. Surprisingly, Ki67 immunoreactivity is restricted to hypertrophic vessels and the cells noted within the lesions did not exhibit strong Ki67 immunoreactivity suggesting that they are now removed from the proliferative phase of development and are residual lesions secondary to the primary inciting cause. Ki67 is a marker for cellular proliferation [53]. Lower grade tumors also have less p53 expression, lower Ki67 index, and fewer microglia compared to higher grade astrocytic tumors (Grade III-IV) [54]. In adult grade II low-grade diffuse glioma, which include diffuse astrocytoma, oligoastrocytoma, and oligodendroglioma, higher Ki67 index correlates with shorter overall patient survival [55]. Another interpretation is that these nodules are part of a neuroprotective response by astrocytes [56]

in slow-progressing animals. However, the organization of the astrocytes into interlacing cells and into coalescing nodules suggests a possible preneoplastic lesion.

The cases presented herein do not have features of an astrocytoma; however with the altered p53 immunoreactivity it suggests that there has been local derangement in astrocyte proliferation and may be a pre-neoplastic change. To our knowledge, this report is the first to describe the histopathologic and immunohistochemical features of perivascular nodular astrocytosis in SIV-immunosuppressed macaques.

Acknowledgments

We are grateful to the veterinary staff at the NEPRC for animal care and the pathology staff for assisting with necropsies and tissue collection, including Meredith Simon and Sherry Klumpp. We thank R.C. Desrosiers, R.P. Johnson, and S. Tzipori for access to brain tissues. We thank Kristen Toohey for graphic support and Susan Alberghini and Katana Queiroli for their administrative assistance. This research was funded, in part, by NIH grants NEPRC Base grant OD0111103 and T32 OD011064.

References

1. Neal JWLM, Morrison HL, Jasani B. Borysiewicz: A malignant astrocytoma in a patient with AIDS: A possible association between astrocytomas and HIV infection. J Infect. 1996; 33:159–162. [PubMed: 8945703]
2. Vannemreddy PSFM, Polin RS, Todd JR, Nanda A. Glioblastoma multiforme in a case of acquired immunodeficiency syndrome: investigation a possible oncogenic influence of human immunodeficiency virus on glial cells. Case report and review of the literature. J Neurosurg. Jan. 2000 92:161–164.
3. Moulignier AMJ, Pialoux G, Eliaszewicz ME, Thurel C, Thiebaut JB. Cerebral glial tumors and human immunodeficiency virus-1 infection. Cancer. 1994; 74:686–692. [PubMed: 8033048]
4. Tacconi L, Stapleton S, Signorelli F, Thomas DG. Acquired immune deficiency syndrome (AIDS) and cerebral astrocytoma. Clinical neurology and neurosurgery. 1996; 98:149–151. [PubMed: 8836588]
5. Gasnault J, Roux FX, Vedrenne C. Cerebral astrocytoma in association with HIV infection. Journal of neurology, neurosurgery, and psychiatry. 1988; 51:422–424.
6. Carrana EJ, Rossitch E, Moore MR, Funkenstein HH. Anaplastic astrocytoma in association with human immunodeficiency virus type 1 infection. The American journal of emergency medicine. 1990; 8:565–567. [PubMed: 2222608]
7. Ho KL, Gottlieb C, Zarbo RJ. Cytomegalovirus infection of cerebral astrocytoma in an AIDS patient. Clinical neuropathology. 1991; 10:127–133. [PubMed: 1650302]
8. Kasantikul V, Kaoroptham S, Hanvanich M. Acquired immunodeficiency syndrome associated with cerebral astrocytoma. Clinical neuropathology. 1992; 11:25–27. [PubMed: 1547579]
9. Wolff R, Zimmermann M, Marquardt G, Lanfermann H, Nafe R, Seifert V. Glioblastoma multiforme of the brain stem in a patient with acquired immunodeficiency syndrome. Acta neurochirurgica. 2002; 144:941–944. discussion 944-945. [PubMed: 12376778]
10. Lakhan SE, Harle L. Difficult diagnosis of brainstem glioblastoma multiforme in a woman: a case report and review of the literature. Journal of medical case reports. 2009; 3:87. [PubMed: 19946563]
11. Ishii T, Mizukawa K, Sasayama T, Sasaki H, Hayashi S, Nakamizo S, Tanaka H, Tanaka K, Hara S, Hirai C, Itoh T, Kohmura E. Immunohistochemical and molecular genetics study of a granular cell astrocytoma: a case report of malignant transformation to a glioblastoma. Neuropathology : official journal of the Japanese Society of Neuropathology. 2013; 33:299–305. [PubMed: 22994265]

12. Crocetti E, Trama A, Stiller C, Caldarella A, Soffietti R, Jaal J, Weber DC, Ricardi U, Slowinski J, Brandes A. Epidemiology of glial and non-glial brain tumours in Europe. Eur J Cancer. 2012; 48:1532–1542. [PubMed: 22227039]
13. Westmoreland SV, Williams KC, Simon MA, Bahn ME, Rullkoetter AE, Elliott MW, deBakker CD, Knight HL, Lackner AA. Neuropathogenesis of simian immunodeficiency virus in neonatal rhesus macaques. The American journal of pathology. 1999; 155:1217–1228. [PubMed: 10514404]
14. Hurley JP, Ilyinskii PO, Horvath CJ, Simon MA. A malignant astrocytoma containing simian virus 40 DNA in a macaque infected with simian immunodeficiency virus. J Med Primatol. Jun.1997 26:172–180. [PubMed: 9379484]
15. Simon MA, Ilyinskii PO, Baskin GB. Association of simian virus 40 with a central nervous system lesion distinct from progressive multifocal leukoencephalopathy in macaques with AIDS. The American journal of pathology. 1999; 154:437–446. [PubMed: 10027402]
16. Geleziunias R, Shipper HM, Wainberg MA. Pathogenesis and therapy of HIV-1 infection of the central nervous system. AIDS. 1992; 6:1411–1426. [PubMed: 1337255]
17. Kleihues P, Burger PC, Scheithauer BW. The new WHO classification of brain tumors. Brain Path. 1993; 3:255–268. [PubMed: 8293185]
18. Hainaut P, Hollstein M. p53 and human cancer: the first ten thousand mutations. Adv Cancer Res. 2000; 77:81–137. [PubMed: 10549356]
19. Network TC. CGAR: Comprehensive genomic characterization defines human glioblastoma genes and core pathways. Nature. 2008; 455:1061–1068. [PubMed: 18772890]
20. Guimaraes DP, Hainaut P. TP53: a key gene in human cancer. Biochimie. 2002; 84:83–93. [PubMed: 11900880]
21. Kim YH, Nobusawa S, Mittelbronn M, Paulus W, Brokinkel B, Keyvani K, Sure U, Wrede K, Nakazato Y, Tanaka Y, Vital A, Mariani L, Stawski R, Watanabe T, De Girolami U, Kleihues P, Ohgaki H. Molecular classification of low-grade diffuse gliomas. The American journal of pathology. 2010; 177:2708–2714. [PubMed: 21075857]
22. England B, Huang T, Karsy M. Current understanding of the role and targeting of tumor suppressor p53 in glioblastoma multiforme. Tumour Biol. 2013; 34:2063–2074. [PubMed: 23737287]
23. Wood D. Long-term mortality and cancer risk in irradiated rhesus monkeys. Radiat Res. 1991; 126:132–140. [PubMed: 1850849]
24. HogenEsch HBJ, Zurcher C. Neurohypophyseal astrocytoma (pituicytoma) in a rhesus monkey (Macaca mulatta). Veterinary pathology. 1992; 29:359–361. [PubMed: 1514223]
25. Ikota H, Kinjo S, Yokoo H, Nakazato Y. Systematic immunohistochemical profiling of 378 brain tumors with 37 antibodies using tissue microarray technology. Acta Neuropathol. 2006; 111:475–482. [PubMed: 16598485]
26. Sprinkle T. 2′,3′-cyclic nucleotide 3′-phosphodiesterase, an oligodendrocyte-Schwann cell and myelin-associated enzyme of the nervous system. Crit Rev Neurobiol. 1989; 4:235–301. [PubMed: 2537684]
27. Cerutti SM, Chadi G. S100 immunoreactivity is increased in reactive astrocytes of the visual pathways following a mechanical lesion of the rat occiptal cortex. Cell Biology International. 2000; 24:35–49. [PubMed: 10826771]
28. Orchard GE. Comparison of immunohistochemical labelling of melanocyte differentiation antibodies melan-A, tyrosinase and HMB 45 with NKIC3 and S100 protein in the evaluation of benign naevi and malignant melanoma. Histochem J. 2000; 32:475–481. [PubMed: 11095072]
29. Bahrami A, Truong LD, Ro JY. Undifferentiated tumor: true identity by immunohistochemistry. Arch Pathol Lab Med. 2008; 132:326–348. [PubMed: 18318577]
30. Pileri SA, Grogan TM, Harris NL, Banks P, Campo E, Chan JK, Favera RD, Delsol G, De Wolf-Peeters C, Falini B, Gascoyne RD, Gaulard P, Gatter KC, Isaacson PG, Jaffe ES, Kluin P, Knowles DM, Mason DY, Mori S, Muller-Hermelink HK, Piris MA, Ralfkiaer E, Stein H, Su IJ, Warnke RA, Weiss LM. Tumours of histiocytes and accessory dendritic cells: an immunohistochemical approach to classification from the International Lymphoma Study Group based on 61 cases. Histopathology. 2002; 41:1–29. [PubMed: 12121233]

31. Ito D, Imai Y, Ohsawa K, Nakajima K, Fukuuchi Y, Kohsaka S. Microglia-specific localization of a novel calcium binding protein, Iba1. Brain Res Mol Brain. 1998; 57:1–9.
32. Naftalian, RJ.; Holman, G. Membrane Transport in Red Blood Cells. Academic Press; London: 1977.
33. Guerin CLJ, Drewes LR, Brem H, Goldsteintlls GW. Vascular expression of glucose transporter in experimental brain neoplasms. The American journal of pathology. 1992; 140:417–425. [PubMed: 1739134]
34. Reisser C, Eichhorn K, Herold-Mende C, Born AI, Bannasch P. Expression of facilitative glucose transport proteins during development of squamous cell carcinomas of the head and neck. Int J Cancer. 1999; 80:194–198. [PubMed: 9935199]
35. Ashton-Sager A, Paulino AF, Afify AM. GLUT-1 is preferentially expressed in atypical endometrial hyperplasia and endometrial adenocarcinoma. Appl Immunohistochem Mol Morphol. 2006; 14:187–192. [PubMed: 16785788]
36. Abbondati E, Del-Pozo J, Hoather TM, Constantino-Casas F, Dobson JM. An immunohistochemical study of the expression of the hypoxia markers Glut-1 and Ca-IX in canine sarcomas. Veterinary pathology. 2013; 50:1063–1069. [PubMed: 23628694]
37. O'Neil SP, Suwyn C, Anderson DC, Niedziela G, Bradley J, Novembre FJ, Herndon JG, McClure HM. Correlation of acute humoral response with brain virus burden and survival time in pigtailed macaques infected with the neurovirulent simian immunodeficiency virus SIVsmmFGb. The American journal of pathology. 2004; 164:1157–1172. [PubMed: 15039205]
38. Sasaki T, Endo T. Both cell-surface carbohydrates and protein tyrosine phosphatase are in volved in the differentiation of astrocytes in vitro. Glia. 2000; 32:60–70. [PubMed: 10975911]
39. Westmoreland SV, Halpern E, Lackner AA. Simian immunodeficiency virus encephalitis in rhesus macaques is associated with rapid disease progression. J Neurovirol. 1998; 4:260–268. [PubMed: 9639069]
40. Sasseville VG, Lackner A. Neuropathogenesis of simian immunodeficiency virus infection in macaque monkeys. J Neurovirol. 1997; 3:1–9. [PubMed: 9147816]
41. Rausch DM, Murray EA, Eiden LE. The SIV-infected rhesus monkey model for HIV-associated dementia and implications for neurological diseases. Journal of Leukocyte Biology. 1999; 65:466–474. [PubMed: 10204575]
42. Axthelm MK, Koralnik IJ, Dang X, Wuthrich C, Rohne D, Stillman IE, Letvin NL. Meningoencephalitis and demyelination are pathologic manifestations of primary polyomavirus infection in immunosuppressed rhesus monkeys. J Neuropathol Exp Neurol. 2004; 63:750–758. [PubMed: 15290900]
43. Hovarth CJ, Simon MA, Bergsagel DJ, Pauley D, King NW, Garcea RL, Ringler DJ. Simian Virus 40-induced disease in rhesus monkeys with simian acquired immunodeficiency syndrome. The American journal of pathology. 1992; 140:1431–1440. [PubMed: 1376560]
44. Kaliyaperumal S, Dang X, Wuethrich C, Knight HL, Pearson C, Mackey J, Mansfield KG, Koralnik IJ, Westmoreland SV. Frequent Infection of Neurons by SV40 Virus in SIV-Infected Macaque Monkeys with Progressive Multifocal Leukoencephalopathy and Meningoencephalitis. The American journal of pathology. 2013; 183:1910–1917. [PubMed: 24095925]
45. Chrétien F, Boche D, Lorin de la Grandmaison G, Ereau T, Mikol J, Hurtrel M, Hurtrel B, Gray F. Progressive multifocal leukoencephalopathy and oligodendroglioma in a monkey co-infected by simian immunodeficiency virus and simian virus 40. Acta Neuropathol. 2000; 100:332–336. [PubMed: 10965804]
46. Baskin G. Disseminated cytomegalovirus infection in immunodeficient rhesus monkeys. The American journal of pathology. Nov.1987 129:345–352. [PubMed: 2823615]
47. Lucas KG, Bao L, Bruggeman R, Dunham K, Specht C. The detection of CMV pp65 and IE1 in glioblastoma multiforme. Journal of neuro-oncology. 2011; 103:231–238. [PubMed: 20820869]
48. Soderberg-Naucler C, Johnsen JI. Cytomegalovirus infection in brain tumors: A potential new target for therapy? Oncoimmunology. 2012; 1:739–740. [PubMed: 22934266]
49. Cesarman E, Mesri EA. Virus associated lymphomas. Curr Opin Oncol. 1999; 11:322–332. [PubMed: 10505767]

50. Kahnt K, Matz-Rensing K, Hofmann P, Stahl-Hennig C, Kaup FJ. SIV-associated lymphomas in rhesus monkeys (Macaca mulatta) in comparison with HIV-associated lymphomas. Veterinary pathology. 2002; 39:42–55. [PubMed: 12102218]
51. Wang F, Rivailler P, Rao P, Cho Y. Simian homologues of Epstein-Barr virus. Philos Trans R Soc Lond B Biol Sci. 2001; 356:489–497. [PubMed: 11313007]
52. Haanstra KG, Wubben JAM, Jonker M, Hart BA. Induction of Encephalitis in Rhesus Monkeys Infused with Lymphocryptovirus-Infected B-Cells Presenting MOG34–56 Peptide. PloS one. 2013; 8:1–11.
53. Scholzen T, Gerdes J. The Ki-67 protein: from the known and the unknown. J Cell Physiol. Mar. 2000 182:311–322. [PubMed: 10653597]
54. Geranmayeh F, Scheithauer BW, Spitzer C, Meyer FB, Svensson-Engwall AC. Graeber: Microglia in gemistocytic astrocytomas. Neurosurg. 2006; 60:159–166.
55. Figarella-Branger D, Bouvier C, de Paula AM, Mokhtari K, Colin C, Loundou A, Chinot O, Metellus P. Molecular genetics of adult grade II gliomas: towards a comprehensive tumor classification system. Journal of neuro-oncology. 2012; 110:205–213. [PubMed: 22890969]
56. London A, Itskovich E, Benhar I, Kalchenko V, Mack M, Jung S, Schwartz M. Neuroprotection and progenitor cell renewal in the injured adult murine retina requires healing monocyte-derived macrophages. The Journal of experimental medicine. 2011; 208:23–39. [PubMed: 21220455]

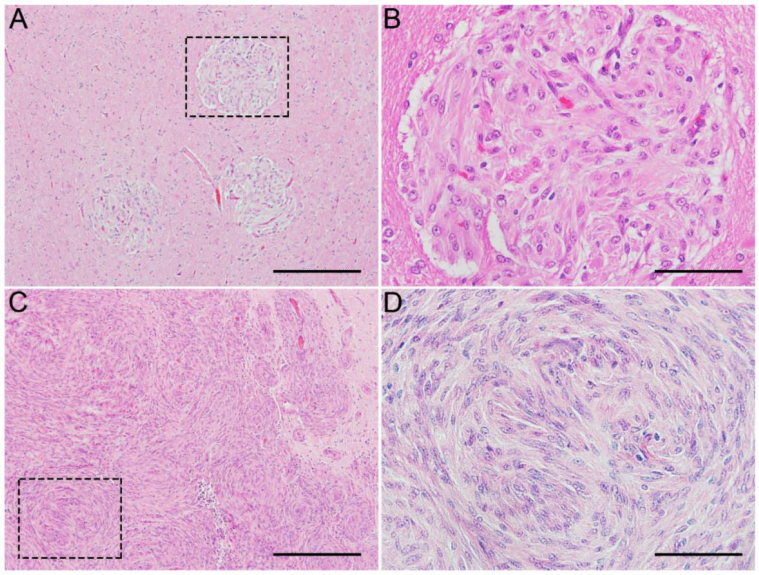

Figure 1.

Brain, rhesus macaques (Macaca mulatta). Multifocal perivascular nodular foci with densely cellular, interlacing populations of elongated spindle cells with abundant eosinophilic cytoplasm. Case 2: Representative nodules, 200 μm in diameter (A). Dashed box indicates enlarged area that shows a single nodule (B). Case 3: Nodules coalesce to form a mass five mm in diameter (C). Dashed box indicates enlarged area that shows nodule (D). Scale bar = 200 μm (A, C) and 50 μm (B, D).

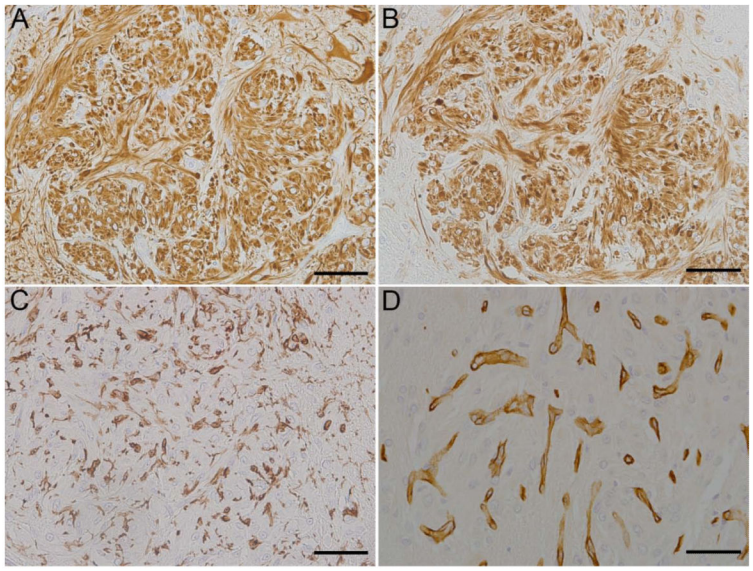

Figure 2.

Brain, rhesus macaques (Macaca mulatta). Immunohistochemical findings, Case 2. Nodules exhibit strong GFAP immunoreactivity (A) and strong vimentin immunoreactivity (B). The proliferative nodules are infiltrated by numerous reactive microglia (C). Glut-1 immunoreactivity is localized to small capillaries (D). Scale bar = 50 μm.

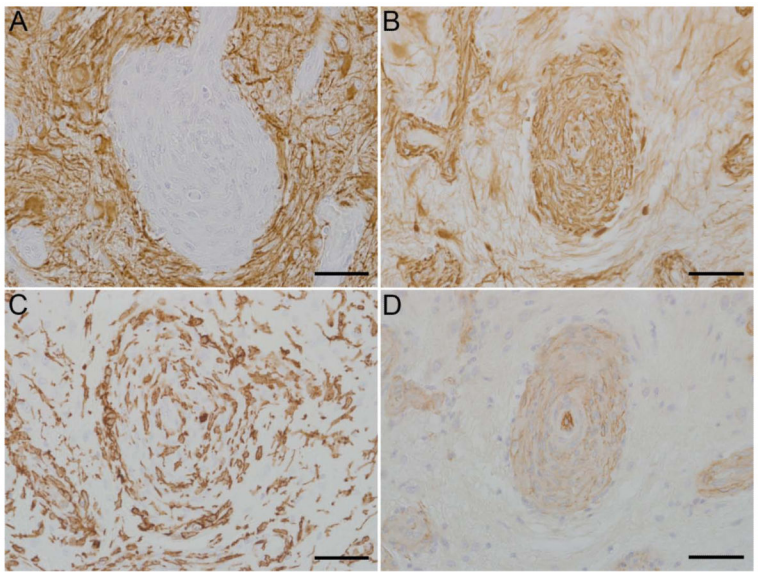

Figure 3.

Brain, rhesus macaques (Macaca mulatta). Immunohistochemical findings, Case 3. There are gemistocytic astrocytes surrounding markedly hypertrophic vessels (A). Hypertrophic vessels exhibit strong vimentin immunoreactivity while the surrounding lesion also displays vimentin immunoreactivity (B). The proliferative lesions and hypertrophic vessels are infiltrated by numerous reactive microglia (C). There is profound endothelial hyperplasia of the vessels found within the lesions (D). Scale bar = 50 μm.

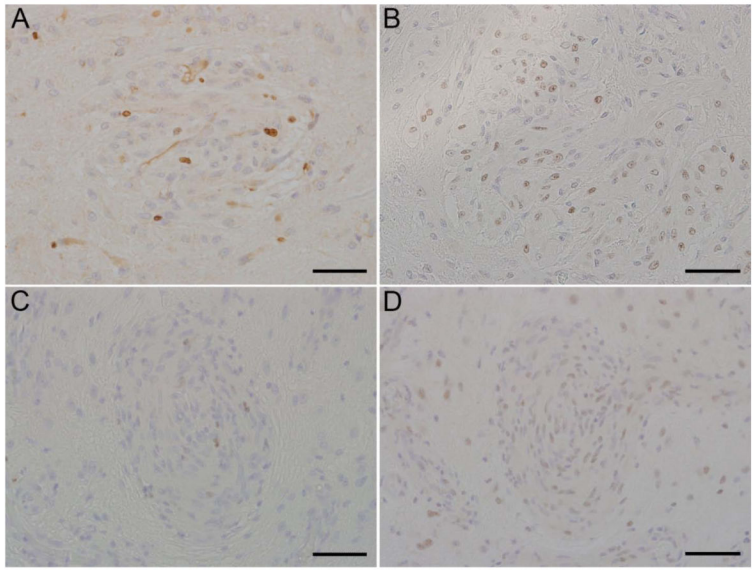

Figure 4.

Brain, rhesus macaques (*Macaca mulatta*). Case 2 (A, B) and Case 3 (C, D). Limited Ki67 immunoreactivity (A, C), and extensive p53 immunoreactivity (B, D). Scale bar = 50 μm.

Table 1

Nodular astrocytosis in SIV-infected rhesus macaques.

Case[1]	Sex	Age	SIV variant (inoculation route)	Days post SIV (first inoculation)	SAIDS	Location of nodular astrocytosis	Neurologic signs[2]	Diameter of representative nodule (μm)
1	M	adult	SIVmac239g46 (iv)	624	+	Cerebral cortex (frontal, temporal, occipital), cerebellum, brainstem	Present	100-200
2	F	8 yr	SIVmac239Δnef (iv, ip)	2,080	+	Cerebral cortex, cerebellum	None noted	300-800
3	M	4 yr	SIVmac239 (iv)	639	+	Cerebral cortex	None noted	100-200
4	F	10 yr	SIVmac239Δnef (iv), SIVmac251 (intravaginal)	1,777	−	Globus pallidus	None noted	200
5	F	5 yr	SIVmac251 (intravaginal)	338	+	Frontal cortex, thalamus, cerebellum	Advanced	100-200

[1] 1,206 total cases (0.4% incidence)

[2] including head tilt, ataxia, falling off of perch, etc.

Table 2

Antibody source, dilution, and antigen retrieval for immunohistochemistry protocols.

Marker	Epitope Retrieval	Primary Antibody	Incubation Time	Dilution	Secondary Antibody	Dilution (all 20 min)	Tertiary Antibody (all 30 min)
GFAP	None	PAH[1], Dako (Carpinteria, CA)	45 min, room temperature	1:340	GAR-b[2]	1:200	Vectastain ABC Elite[3]
Vimentin	Proteinase K (5 min, RT)	MAH[4], Clone 3B4, Dako	Overnight, 4°C	1:162	HAM-b[5]	1:200	Vectastain ABC Standard[3]
Glut-1	Microwave[6]	PAH[1], Millipore (Billerica, MA)	30 min, room temperature	1:1000	GAR-b[2]	1:200	Vectastain ABC Standard[3]
CNPase	Microwave[6]	MAH4, Clone 11-5B, NeoMarkers (Fremont, CA)	60 min, room temperature	1:200	HAM-b[5]	1:200	Vectastain ABC Elite[3]
S100	Microwave[6]	PAH1, S100, Dako	60 min, room temperature	1:3200	GAR-b[2]	1:200	Vectastain ABC Elite[3]
Iba1	Microwave[6]	PAH[1], Wako (Richmond, VA)	30 min, room temperature	1:1000	GAR-b[2]	1:200	Vectastain ABC Elite[3]
Ki67	Microwave[6]	MAH[4], Clone MIB-1, Dako	Overnight, 4°C	1:35	HAM-b[5]	1:200	Vectastain ABC Elite[3]
p53	Microwave[6]	MAH[4], Clone DO-7, AbD Serotec (Raleigh, NC)	Overnight, 4°C	1:500	Dual Link System, Dako	None	None
SIV	Microwave[6]	MAH[4], HIV-1 p24[7]	Overnight, 4°C	1:400	HAM-b[5]	1:200	Vectastain ABC Elite[3]
SV40	Microwave[6]	MAH[4], SV40 large T antigen, Clone Pab416, Oncogene (Billerica, MA)	Overnight, 4°C	1:25600	HAM-b[5]	1:200	Vectastain ABC Elite[3]
CMV	Microwave[6]	serum, CMV, IEI (exon4), PA Barry, UCD-CCM (Davis, CA)	30 min, room temperature	1:1600	GAR-b[2]	1:200	Vectastain ABC Standard[3]
LCV	Microwave[6]	MAH[4], EBNA2, Clone PE2, Leica (Buffalo Grove, IL)	Overnight, 4°C	1:600	HAM-b[5]	1:200	Vectastain ABC Elite[3]

[1] Polyclonal anti-human

[2] Biotinylated goat anti-rabbit, Vector Laboratories, (Burlingame, CA, USA)

[3] Vector Laboratories

[4] Monoclonal anti-human

[5] Biotinylated horse anti-mouse, Vector Laboratories

[6] Microwave in sodium citrate buffer for 20 minutes, followed by cooling at room temperature for 20 minutes

[7] The following reagent was obtained through the NIH AIDS Research and Reference Reagent Program, Division of AIDS, NIAID, NIH: HIV-1 p24 Monoclonal Antibody (183-H12-5C) from Dr. Bruce Chesebro and Kathy Wehrly.

Table 3

Immunohistochemistry of nodular lesions in SIV-infected rhesus macaques for cellular markers and viral antigens.

Case No.	GFAP	Vimentin	S100	Glut-1	CNPase	Iba1	SV40	CMV	LCV
1	+	+	+	−	−	−	−	−	−
2	+	+	+	−	−	−	−	−	−
3	−	+	+	−	−	−	−	−	−
4	+	+	+	−	−	−	−	−	−
5	+	+	+	−	−	−	−	−	−

Table 4

Percentage of immunoreactive nuclei within nodular lesions in SIV-infected rhesus macaques for indices of cellular proliferation and cell cycle control. Average of five lesions.

Case No.	Ki67	P53
1	0%	Not tested
2	<5%	>90%
3	10%	>90%
4	<5%	>90%
5	<5%	>90%